INFLUENCE OF THE CYLINDER DIAMETER VARIATION ON THE NEAR WAKE BEHAVIOUR IN UNIFORM FLOW

H. Oualli

Fluid Mechanics Laboratory, EMP, Bordj El Bahri, Algiers, ALGERIA

S. Hanchi

Fluid Mechanics Laboratory, EMP, Bordj El Bahri, Algiers, ALGERIA

A. Bouabdallah

LTSE, Université des Sciences et de la Technologie (USTHB), Algiers, ALGERIA

R. Askoviç

LME, UVHC, Valenciennes, FRANCE

ABSTRACT

This study presents a numerical and experimental investigation of an active controlling technique of the flow around a radially pulsating circular cylinder. The computations and experiments are performed for a relatively wide range of the Reynolds number from Re=300 up to 30×10^3. The validity of the proposed technique is thus assessed for both moderately low and high Reynolds numbers.

It is particularly focused on the drag coefficient behavior when the cylinder is superimposed to radial oscillations. The flow response is investigated when the deforming amplitude is fixed equal to 5% the value of the initial cylinder radius and the forcing Strouhal number St_f is varied over the range ($0 \le St_f \le 2$).

It is shown that, for a sufficiently high Reynolds number and a suitable value of the applied vibrating frequency the drag coefficient drops to reach negative values inducing the propulsion of the cylinder.

In addition, the characterizing topology of the corresponding flow regimes is accompanied by strong modifications—in the near wake and along the Von Kármán eddy street—in response to the actuating technique.

1. INTRODUCTION

The problem of Fluid Induced Vibration, FIV, is a highly specialized subject in which numerous disciplines imbricate incorporating fluid mechanics, structural mechanics, vibrations, computational fluid dynamics, acoustics, statistics, smart materials…as discussed in Zdravkovich (1981) and Sarpkaya (2004) reviews. Such problems can occur in many engineering situations: bridges, stacks, transmission lines, aircraft control surfaces, offshore structures, heat exchangers, marine cables, towed cables, pipelines and other hydrodynamic and hydroacoustic applications. Much of the research into flow induced vibrations has been dedicated to the problem of a cylinder vibrating in line or transversely to a fluid flow. There are very few papers devoted to studying the case of a radial vibration where there is a uniform variation of the cylinder cross-section along the whole span of the body.

Here, we set out to study the dynamics and vortex formation for a controlled cylinder, which is able to vibrate in the radial direction—variation of the cross-section diameter—according to a previously fixed sinusoidal law.

2. NUMERICAL METHOD

We perform simulations of an unsteady flow around a circular cylinder with a uniformly sinusoidal deforming function of the radius according to the following law:

$$\frac{a}{a_0} = 1 + \frac{a_m}{a_0}\sin\left(2\pi St_f\, t\right) \qquad (01)$$

where a and a_0 are respectively the instantaneous and initial radii of the cylinder, St_f is the forcing Strouhal number imposed to the cylinder, a_m the maximum amplitude and t is time .

The cylinder is impulsively started into rectilinear motion with a constant infinite velocity U_∞ in a two-dimensional viscous incompressible fluid flow initially at rest. The Navier-Stokes equations are solved in stream function-vorticity formulation using polar coordinates. The turbulence effect is determined using the Smagorinsky subgrid scale model. Several simulations of flows around the cylinder have been performed in order to validate the numerical method, Hanchi et al. (2004).

An LES method is used to represent the wake turbulence at Re=300. The approach used to

calculate the flow field is the same as that in Hakizumwami (1994) and Al-Jamal et al. (2004) with differences to be described later. The finite difference scheme serves as a natural filtering operator with a filter width that is the local grid size. The filtered 2-D governing equations are the Poisson equation for the stream function ψ,

$\Delta^2\psi=-\omega$ (2)

and the vorticity transport equation,

$$\frac{\partial\omega}{\partial t_1}+u\frac{\partial\omega}{\partial r}+\frac{v}{r}\frac{\partial\omega}{\partial\theta}=(\nu+\nu_t)\left(\frac{\partial^2\omega}{\partial r^2}+\frac{1}{r}\frac{\partial\omega}{\partial r}+\frac{\partial^2\omega}{\partial\theta^2}\right) \quad (3)$$

where

$$u=\frac{1}{r}\frac{\partial\psi}{\partial\theta},\ v=-\frac{\partial\psi}{\partial r} \text{ and } \omega=\frac{1}{r}\frac{\partial(rv)}{\partial r}-\frac{1}{r}\frac{\partial u}{\partial\theta} \quad (4)$$

r and θ are the dimensional coordinates in the physical plane, t_1 is the dimensional time, ν is the kinematic viscosity of the evolving fluid, ν_t is the turbulent eddy viscosity, u and v are the radial and circumferential velocity components, and ω is the vorticity. All of the flow variables are the large scale (resolvable) quantities.

The effects of turbulence are taken into account by the eddy viscosity ν_t , which is determined by a subgrid scale model. In the present computations, we use the Smagorinsky model,

$$\nu_t=(C_s\Delta)^2\sqrt{2S_{ij}S_{ij}} \quad (5)$$

C_s is the Smagorinsky constant, Δ is the length scale (taken here to be the local mesh size) and S_{ij} is the strain rate tensor.

The initial cylinder diameter D_0 and the infinite velocity U_∞ are selected as length and velocity scales, respectively, with the non dimensional time $t = t_1 U_\infty / D_0$. The non dimensional governing equations are:

$$\frac{\partial\omega}{\partial t}+u\frac{\partial\omega}{\partial r}+\frac{v}{r}\frac{\partial\omega}{\partial\theta}=\left(\frac{2}{\mathrm{Re}}+\frac{2}{\mathrm{Re}_t}\right)\nabla^2\omega \quad (6)$$

and

$$\nabla^2\psi=-\omega \quad (7)$$

where $\nabla^2=\frac{\partial^2}{\partial r^2}+\frac{1}{r}\frac{\partial}{\partial r}+\frac{\partial^2}{\partial\theta^2}$ is the Laplacian operator and ψ is the streamfunction.

Considering the non dimensional quantities:

$$r=\frac{r_1}{D_0}=k(\xi)=\alpha e^{\xi}+\beta,\ \mathrm{Re}=\frac{U_\infty D_0}{\nu},\ t=\frac{t_1 U_\infty}{D_0},\ St_f=\frac{f_S D_0}{U_\infty}$$

$$\tilde{\psi}=\frac{\psi}{U_\infty D_0},\ \omega=\frac{\omega D_0}{U_\infty},\ \mathrm{Re}_t=\frac{U_\infty D_0}{\nu_T},\ \beta=1-\alpha,\ 0<\alpha<1$$

St_f is the forcing Strouhal number and fs the dimensional cylinder shedding frequency.

The initial conditions: $\tilde{\psi}=0$ and ω = 0 at t = 0

The boundary conditions:

$$\xi=0:\quad u_1=\frac{\partial a}{\partial t_1} \text{ and } v_1=0$$

$$\zeta\to\infty:\quad \tilde{\psi}=\left(k(\xi_\infty)-\frac{1}{k(\xi_\infty)}\right)\sin(\theta)-\frac{\theta}{k(\xi_\infty)}\frac{\partial f_s}{\partial t}$$

The new system to resolve is then:

$$\frac{\partial\omega}{\partial t}=\frac{\omega}{1+f_s}\frac{\partial f_s}{\partial t}+G \quad (08)$$

$$\omega=\left(\frac{\partial k}{\partial\xi}\right)^{-2}\left(\frac{\partial^2\psi}{\partial\xi^2}\right)+k^{-2}\left(\frac{\partial^2\psi}{\partial\theta^2}\right)+\left(k^{-1}\left(\frac{\partial k}{\partial\xi}\right)^{-1}-\left(\frac{\partial^2 k}{\partial\xi^2}\right)\left(\frac{\partial k}{\partial\xi}\right)^{-3}\right)\frac{\partial\omega}{\partial\xi}$$

where,

$$G=\frac{k^{-1}\left(\frac{\partial k}{\partial\xi}\right)^{-1}}{1+f_s}\left[\frac{\partial\omega}{\partial\xi}\left(\frac{\partial\psi}{\partial\theta}-k(0)\frac{\partial f_s}{\partial t}\right)-\frac{\partial\omega}{\partial\theta}\frac{\partial\psi}{\partial\xi}\right]$$

$$+\frac{1}{1+f_s}\left(\frac{2}{\mathrm{Re}}+\frac{2}{\mathrm{Re}_t}\right)\times\left(\left(\frac{\partial k}{\partial\xi}\right)^{-2}\frac{\partial^2\omega}{\partial\xi^2}+k^{-2}\frac{\partial^2\omega}{\partial\theta^2}+\left(k^{-1}\left(\frac{\partial k}{\partial\xi}\right)^{-1}-\left(\frac{\partial^2 k}{\partial\xi^2}\right)\left(\frac{\partial k}{\partial\xi}\right)^{-3}\right)\frac{\partial\omega}{\partial\xi}\right)$$

with the new boundary conditions set

ξ = 0, ψ = 0 (09)

ξ→∞

$$\psi=\left(k(\xi_\infty)-\frac{1}{k(\xi_\infty)}\right)\sin(\theta)-\frac{\theta}{k(\xi_\infty)}\frac{\partial f_s}{\partial t}+k(0)\frac{\partial a}{\partial t}\theta \quad (10)$$

and

$$\frac{\partial\omega}{\partial t}=\frac{\omega}{1+f_s}\frac{\partial f_s}{\partial t}+\frac{k^{-1}\left(\frac{\partial k}{\partial\xi}\right)^{-1}}{1+f_s}\left[\frac{\partial\omega}{\partial\xi}\left(\frac{\partial\psi}{\partial\theta}-k(0)\frac{\partial f_s}{\partial t}\right)-\frac{\partial\omega}{\partial\theta}\frac{\partial\psi}{\partial\xi}\right] \quad (11)$$

This set of the governing equations is resolved in a polar grid geometry and the parameters for the radial coordinate are taken as in Justesen (1991)

$r=0.6e^{\zeta}+0.4$

The following equations illustrate the drag coefficient in its components, skin and pressure drag computed as in Koumoutsakous et al. (1995). It is important to note that the drag force is directly linked to the forcing Strouhal number St_f.
The pressure drag is given by:

$$F_p = -\int_0^{2\pi} \left(\frac{2}{\mathrm{Re}} \frac{\partial \omega}{\partial \xi} + \left(\frac{\partial \psi}{\partial \theta} - \frac{1}{a_0} \frac{\partial a}{\partial t} \right) \omega \right) e_\theta \, d\theta \qquad (14)$$

The friction drag is computed from the vorticity on the cylinder surface as:

$$F_f = \int_0^{2\pi} \left(\frac{2\omega}{\mathrm{Re}} \right) e_\theta \, d\theta \qquad (15)$$

The total drag force on the body is thus:

$$F_T = F_p + F_f \qquad (16)$$

The total drag coefficient of the body is evaluated by

$$C_D = \frac{F_T \bullet e_x}{U_\infty{}^2 a} \qquad (17)$$

where ω is the vorticity, ζ and θ are the polar coordinates in the computational field and ψ is the streamfunction.

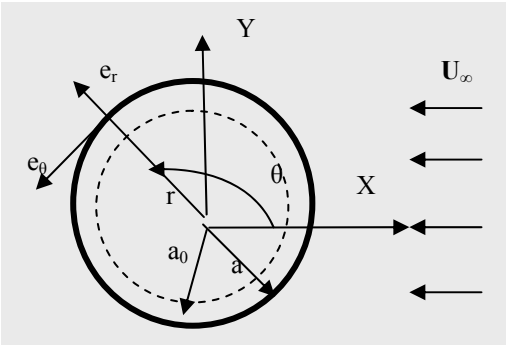

Figure 1: Cylinder schematic sketch

The validation of the computational method is executed, as suggested by Koumotsakos et al. (1995), using drag coefficient results rather than the streamlines configurations. Vorticity is expressed in second order derivatives of the velocity components, allowing thus detection of smaller scale variations which can be imperceptible in streamline patterns.
For Re=550, fig. 2 and 3, our results correlates satisfactorily with those of Koumotsakos et al. (1995).

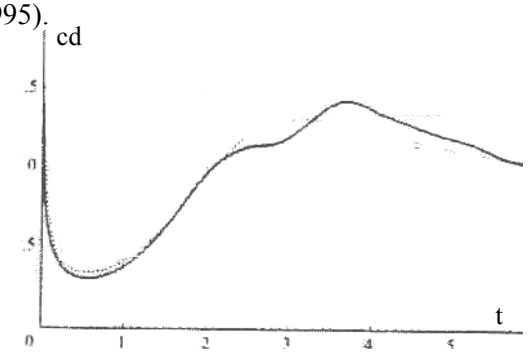

Figure 2: Time evolution of the drag coefficient around an impulsively started circular cylinder for Re = 3000, Koumoutsakos and Leonard (1995)

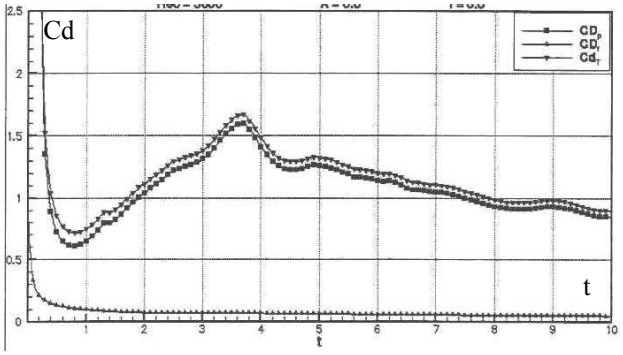

Figure 3: Time evolution of the drag coefficient around an impulsively started circular cylinder for Re=3000 (Present study).

3. EXPERIMENTAL SETUP

These experiments are carried out in an open circuit channel facility EV 280 type. It consists of a low speed air turbine (0.3 - 3 m/s) with a large Plexiglas tunnel, approximately 1.5 m long, 0.35m height and 0.45 wide with optical access from all sides. The background streamwise disturbance level is less than 1% of the free stream velocity.
The cylinder made of PVC (Polyvinyl Chlorine), fig. 4, is mounted horizontally traversing the test section with one end linked to an external motor destined to deliver rotating motion of the cylinder shaft. The inside of the test cylinder, as shown by fig. 4, consists of the cylinder shaft entrained in rotation motion (by means of the external motor), rotating cams appropriately transform the rotating

motion into diameter variation movement of the test cylinder walls according to the equation (01).

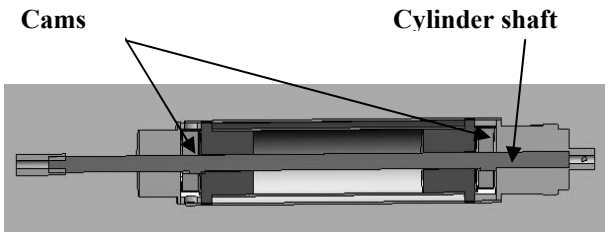

Figure 4: Operating setup / Cylinder deforming mechanism

Considering the cylinder dimensions, this law becomes:

$$a = 0.04\,(1+\left|\,0.005\sin\,(2\pi\times St_f\times t)\,\right|) \qquad (18)$$

Flow is thus controlled by the sinusoidal variation of the radius a. The internal deforming system of the cylinder and the test section dimensions imposed an aspect ratio of 5.62. The flow visualizations are carried out by releasing a horizontal smoke sheet in front of the cylinder created by injecting smoke through a tubing of a smoke generator enabling a steady leakage of smoke through the oncoming flow.

The collection of flow visualization images is taken with a digital video camera. The rotating movement is generated by an electrical motor developing a rotation speed N varying from de 0 to 300 rpm. The cylinder axis is clamped to an electrical motor and constrained to move in a rotating motion to generate the vibrating dynamic of the cylinder cross section via the integrated mechanism inside the cylinder. The rotating cams convert the rotary motion of the drive shaft into sinusoidal motion of cylinder walls by an appropriate mechanism, fig.4.

With this system, the corresponding forcing Strouhal number, $St_f = f\,D/U_\infty$, extends in the range from 0.7 to 15. D and U_∞ are respectively the cylinder diameter and the infinite flow velocity.

Flow visualizations are carried out to study the behavior of the cylinder near wake in response to the radial vibration controlling techniques.

The present investigation of the near wake of a circular cylinder superimposed to diameter variation is an initial step towards understanding the intricate flow phenomena generated when such an active controlling technique is applied to a flow around a circular cylinder.

4. RESULTS AND DISCUSSION

A radial wave generated by the wall motion is forced to propagate from the surface of the cylinder to reach the outer flow as depicted in the figure 6. This wave, when travelling radially from the cylinder surface to the outer flow, fig. 6, is expected to modulate the instantaneous values of the streamwise and transverse velocity components u and v as illustrated by the fig. 5. The velocity time histories are shown for a cylinder mid span point located at 10D downstream. The modulated character of the velocity shows clearly the expanded influence of the pulsatile motion of the cylinder walls to the different cylinder surrounding regions (wake, shear layers, retarded flow).

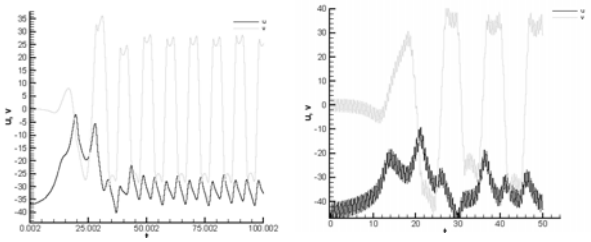

Figure 5: Velocity time histories for Re = 500
(a) non controlled case
(b) controlled case with St_f=2

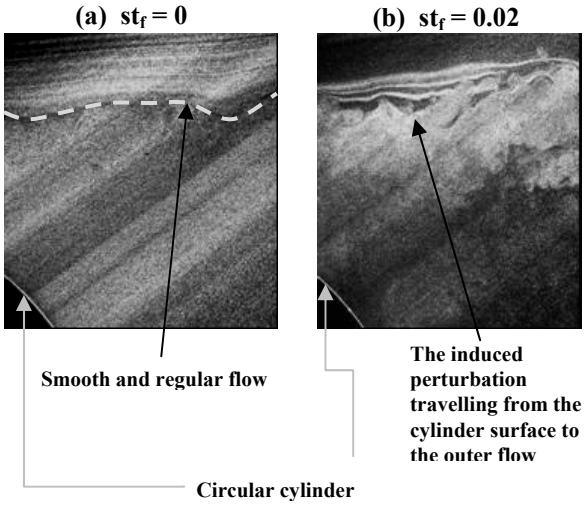

Figure 6: Visualisation of the flow around a circular cylinder for $Re=20\times10^3$

The boundary layer is subject to the walls vibration mode via the flow disturbance forcing function acting as an active vibrating damper. The flow instabilities are thereby excited and the flow destabilization, in this case, may be subsequent to the altered phase relation in the shedding mechanism of the Von Kármán eddies.

The steady state stability theory led to the fact that wall displacement will induce a traveling pressure signal that, in turn, will modulate the mean velocity

profile. This is in line with the velocity time histories observed from the present computations, fig. 5.
Oualli et al. (2004, 2007) considered in detail the primary and secondary vortices interplay. It is established that the diameter increasing-decreasing motion profoundly affect the shedding mechanism in such a way that the secondary vortices are continuously forced to cut links between the Kármán vortices and the body. These vortices are thus forced to disengage prematurely from the cylinder before reaching the scale and strength of the natural case. The cylinder wake dimensions are thus reduced as well as the scale and strength of the shed structures. This is expected to be the underlying phenomenon responsible of the substantial drag reduction revealed by the numerical computations, fig. 7.

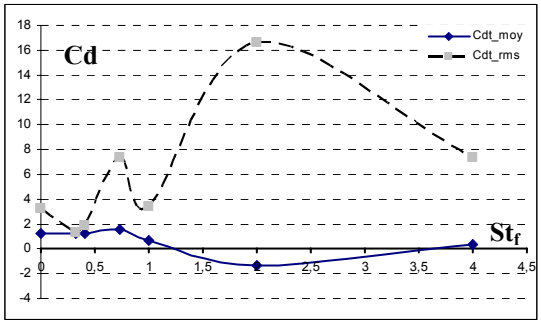

Figure 7: Evolution of the mean and rms values of the drag coefficient around a controlled cylinder versus the applied frequency, Re = 500.

In fact, when the forcing Strouhal number reaches, $St_f \approx 1.25$, the mean value of the drag coefficient, Cd, becomes negative while the root mean square value increases correspondingly until St_f is equal to 3.5. Over this threshold value, the drag coefficient evolves again to positive values.

5. CONCLUSION

The flow characteristics of the near wake and the shedding mechanism behind an actively controlled circular cylinder are numerically and experimentally investigated. The controlling technique is applied over a wide range of the forcing Strouhal numbers.
Flow visualizations are performed and ensured the ability of the generated perturbations to reach the outer flow via the boundary layer and the near wake flow.
The controlling technique is found to influence all the parameters on which the turbulent shedding mode is identified to depend on. A correct adjustment of the controlling parameters, specifically the amplitude and the frequency of vibration, allows avoiding the occurrence of the aerodynamic synchronization and lock-in phenomena.
The drag coefficient around the circular cylinder is expected to be subject of a drastic decreasing and negative values can be reached for a relatively wide range of the forcing Strouhal number.
Further investigations need to be carried out in order to quantify accurately the induced modifications.

6. REFERENCES

Zdravkovich, M. M., Review and classification of various aerodynamic and hydrodynamic means for suppressing vortex shedding. *Journal of fluid and Engineering and Industrial Aerodynamics,* **7:** 145-189.

Sarpkaya, T., 2004, A critical review of the intrinsic nature of vortex induced vibrations. *Journal of Fluids and Structures*, **19**: 389-447.

Hanchi, S., Oualli, H., Bouabdallah, A., Askoviç, R., 2003, Numerical Simulation and Experimental Visualization of the Influence of the Deformation Frequency of a Radially Deforming Circular Cylinder Impulsively Started on Cylinder Wake. Int. J. Num. Meth. Fluids, **41:** 905-930.

Hakizumwami, B. K., 1994, High Reynolds number flow past an impulsively started circular cylinder. computers Fluids **23:** No. 7, 895-902.

Al-Jamal, H., Dalton, C., 2004, Vortex induced vibrations using large eddy simulation at a moderate Reynolds number. Journal of Fluids and Structures, **19:** 73-92.

Justesen, P., 1991, A numerical study of oscillating flow around a circular cylinder. Journal of Fluid Mechanics **222:** 157-196.

Koumotsakos, P., Leonard, A., 1995, High-Resolution Simulations of the Flow Around an Impulsively Started Cylinder Using Vortex Method. J. Fluid Mech. **196:** 1-38.

Oualli, H., Hanchi, S., Bouabdallah, A., Askoviç, R., 2004, Experimental investigation of the flow around a radially vibrating circular cylinder. Experiments in fluids, **37:** 789-801.

Oualli, H., Hanchi, S., Bouabdallah, A., Askoviç, R., Gad-El-Hak, M., 2008, Interaction between the near wake and the cross-section variation of a circular cylinder in uniform flow. Experiments in fluids, (in press).